JAST (Journal of Animal Science and Technology) TITLE PAGE
Upload this completed form to website with submission

ARTICLE INFORMATION	Fill in information in each box below
Article Type	Research article
Article Title (within 20 words without abbreviations)	Caecum transcriptome and associated microbial community in young calves with artificial dosing of rumen content obtained from an adult cow
Running Title (within 10 words)	Caecum transcriptome and associated microbial community in young calves
Author	Wenli Li[1*], Brianna Murphy[2, 3] and Anna Larsen[2, 3]
Affiliation	1. US Dairy Forage Research Center, Agricultural Research Service, USDA, 1925 Linden Drive, Madison, WI 53706 2. Oak Ridge Institute for Science and Education, 1299 Bethel Valley Rd, Oak Ridge, TN 37830 3. Department of Animal and Dairy Sciences, University of Wisconsin-Madison, 1675 Observatory Dr, Madison, WI 53706
ORCID (for more information, please visit https://orcid.org)	Wenli Li (https://orcid.org/0000-0002-9006-0634) Brianna Murphy (https://orcid.org/0009-0002-1762-6379) Anna Larsen (https://orcid.org/0000-0001-6749-6133)
Competing interests	No potential conflict of interest relevant to this article was reported.
Funding sources State funding sources (grants, funding sources, equipment, and supplies). Include name and number of grant if available.	The funding for this experiment is provided by projects 5090-31000-024 and 5090-31000-026 from USDA Agricultural Research Service, US Department of Agriculture. This research used resources provided by the SCINet project and the AI Center of Excellence of the USDA Agricultural Research Service, ARS project number 0500-00093-001-00-D.
Acknowledgements	We thank Andrea Edwards for helping with the tissue sample processing and cataloging. The farm crew at the US Dairy Forage Research Center helped with day-to-day calf management.
Availability of data and material	Upon reasonable request, the datasets of this study can be available from the corresponding author.
Authors' contributions Please specify the authors' role using this form.	Conceptualization: Wenli Li Data curation: Anna Larsen and Wenli Li Formal analysis: Wenli Li and Anna Larsen Methodology: Wenli Li, Anna Larsen and Brianna Murphy

	Software: Wenli Li Validation: Anna Larsen and Wenli li Investigation: Wenli Li Writing - original draft: Wenli Li and Anna Larsen Writing - review & editing: Wenli Li, Anna Larsen and Brianna Murphy
Ethics approval and consent to participate	This article has IACUC approval for animal experiment.

CORRESPONDING AUTHOR CONTACT INFORMATION

For the corresponding author (responsible for correspondence, proofreading, and reprints)	**Fill in information in each box below**
First name, middle initial, last name	Wenli Li
Email address – this is where your proofs will be sent	wenli.li@usda.gov
Secondary Email address	
Address	1925 Linden Drive, Madison, WI, 53706, US
Cell phone number	01-9206505542
Office phone number	01-6088900056
Fax number	

(Unstructured) Abstract (up to 350 words)

Nutritional studies in the cattle typically focus on the rumen and its microbial environment, leaving other parts of the gastrointestinal (GI) tract largely unexplored. Thus, underlying molecular mechanisms and the responses to dietary treatment in the lower gut is poorly understood. In this study, we investigated the caecum transcriptome changes and its associated microbial communities in calves with or without artificially dosed rumen content extracted from an adult cow. Eight calves were included in the study, four received artificially dosed adult rumen content (Treated) and the rest received autoclaved rumen content as a control. We observed significant transcriptome changes in the caecum between treatments, with 1,836 differentially expressed genes (DEGs) identified. A predominant portion of the DEGs were down-regulated in the treated group, which showed significant enrichment for molecular pathways related to immune response, host response to pathogens, and inflammatory responses. For the DEGs correlated with the highest number of microbes, gene ontology analysis indicated an enrichment in pathways associated with inflammation and immune response. By comparing the microbial taxa abundance among different GI tissues collected from the same study, we observed that the same dosing strategy may lead to differential retention of the microbial community in different GI tract locations. Our work indicated that the hind gut showed robust response to artificial dosing and the caecum microbial community may interact extensively with the host to shape the development and maturity of the host immune system in early life. Furthermore, our analysis suggested that tissue-specific analysis is required to fully understand the impact of early dosing on animal performance and physiology.

Keywords (3 to 6):

early dosing, calf caecum, transcriptome changes, microbial community

Introduction

Calves were born with an under-developed rumen. Rumen development is accompanied by gut microbial colonization (1). Feed-induced rumen development has been a key target in calf nutrition, with studies showing an early feeding regime and nutritional strategies can promote early rumen development and the establishment of microbial communities (2). Additionally, studies indicated that microbial community changes induced through early feeding strategies may persist for 4-5 months (3, 4). Direct feeding of microbes, probiotics, and prebiotics at the weaning period, to manipulate the gut microbiota, have yielded positive results in facilitating the rumen microbial development (5-8). Thus, neonatal period was considered an opportune window for rumen microbial manipulation (9-11).

The beneficial role of rumen content dosing was realized long before the extensive studies in ruminal microbiome using sequencing technologies. For example, artificial dosing of rumen content of a healthy cow was practiced to treat a sick recipient animal (12), and rumen transfaunation was evaluated for the treatment of indigestion (13) and abomasum displacement in cattle (14). In early weaned lambs, inoculation of fresh adult rumen fluid into the rumen improved average daily gain and digestibility (15). In our recently published work, we inoculated the rumen content extracted from an adult cow into the young calves from birth to 8 weeks of age. We observed significant changes in the liver transcriptome along with distinctive microbial communities in the rumen epithelial (16), abomasum (17) and ileum (18) in the calves subjected to early dosing compared to the control animals. Taken together, these studies suggest that artificial dosing of rumen content in neonatal ruminants may offer an effective approach to elicit microbial changes in the gut.

In ruminants, both the rumen and hindgut play significant roles in feed fermentation. However, nutritional studies in cattle primarily focus on the rumen and its microbial environment, leaving the molecular mechanisms and the responses to dietary treatment in the

hindgut poorly understood. Previous work indicated that some important vitamins were provided by microbial fermentation in the hindgut, such as vitamin K, thiamine and riboflavin (19, 20). In dairy cattle, hind-gut microbial fermentation is generally responsible for 5 to 10% of total-tract carbohydrate digestion (reviewed in (21)). As part of the hind gut, caecum is the first region of the large intestine, which is a pouch area, where the large and small intestine meet. In lambs, the cecum has a reported role in breaking previously undigested fiber, and producing ~6-14% of the short-chain fatty acids (22). In the large bowel and caecum of the cow, the fermentable substrates are limited. These substrates include lignin, crystalline starches unprocessed during foregut digestion and absorption, and some secreted mucins (23). When dairy cows are fed concentrate-rich diets, large amounts of starch are fermented in the large intestine, leading to hindgut dysbiosis (24, 25). The buffering capacity in the hindgut is limited since it lacks saliva, making the hindgut more susceptible to compromised mucosal permeability and integrity (26).

Like the rumen, microbial colonization in the lower gut occurs after birth. In tangent, the mechanisms governing development and function in the gut change with the microbial community. Few studies investigated the microbial communities in the cecum. Cecal and rumen microbial communities differ in composition and abundance (27). This difference might be explained by the fermentable substrates in the caecum, which are different from these in the rumen. Godoy-Vitorino and co-authors compared microbial communities of cow cecum and rumen. They reported that the rumen had higher proportions of Bacteroidetes and Spirochaetes, and lower proportions of Firmicutes (Bacillota) and Proteobacteria (Pseudomonadota) compared to the cecum (28). The cecal microbiota contributes to the post-rumen fermentation of substrates undigested in the rumen. In Holstein steers, cecal fermentation provided up to 8.6% of metabolizable energy intake (29). Thus, the microbial community changes in the caecum has a perceived impact host's metabolism. These studies suggested that methods targeting the hindgut might provide new opportunities for nutrient use improvement. However, we still have scarce

information on the function of the caecum and its microbial community.

In this study, as a part of a larger study, we focus on investigating the caecum transcriptome changes and its associated microbial communities in calves with or without artificially dosed rumen content extracted from adult cow. Additionally, we compared the microbial communities among the rumen, ileum, abomasum, and caecum tissues collected from the same group of calves using rRNA transcripts generated by RNA-sequencing. This systematic, comparative analysis shed light into the impact of artificial dosing of adult rumen content on microbial communities in various locations of the digestive system in young calves.

Materials and Methods

Animals, diets, and management

The animal protocols for both the donor cows and young calves approved by University of Wisconsin-Madison, Institutional Animal Care and Use committee (IACUC). All methods were performed in accordance with the relevant guidelines and regulations**.**

As previously described, two adult cows were used as donor for rumen content preparation as previously identified, they were high milk production efficiency (HE) and low milk production efficiency (LE) cows (30). Pairwise, high- (HE) and low efficiency (LE) adult cows were selected using milk production efficiency index (MPI) to avoid the difficulty in comparing animals with drastically different milk production levels. MPI was calculated by dividing energy-corrected milk (ECM) with dry matter intake (DMI) (31). One adult HE cow (4262; MPI = 1.8, 5 years of age) was selected as the HE donor cow. The pairwise LE cow (4297; MPI = 1.6, 5 years of age) was also identified. The adult cows were offered *ad libitum* access to water and were fed a total mixed ration (TMR) once daily post-morning milking. TMR ingredient composition was to meet nutritional requirements for lactating dairy

cattle established by the National Research Council (32). On on a dry-matter basis, TMR contained 29.2% neutral detergent fiber (NDF; determined following treatment with sodium sulfite and α-amylase), 43.4% non-fiber carbohydrate, 17.1% crude protein, and 5.0% fat. The detailed TMR information is included in previously published work (33). This study was performed according to animal protocol A01104, approved by the IACUC of University of Wisconsin-Madison.

For the calves, experiment was performed according to the animal protocol A01501 approved by IACUC of University of Wisconsin-Madison. Eight bull calves were enrolled at birth and randomly assigned into two groups: Treated, inoculated with rumen content from HE donor cow; and control: inoculated with autoclaved rumen content. Besides inoculation, standard herd practices employed by the United States Dairy Forage Research Center farm were carried out throughout the experiment.

Rumen content sampling, preparation, and dosing

The procedure for preparing the dosing inocula was published previously (16). From the donor cow, fresh ruminal content was removed in the medio-ventral region of the rumen. To make the inoculum, lightly squeezed solids and rumen liquid were mixed by volume in a 3:1 ratio to make the inoculum. The mixture was blended under CO_2 immediately for 1 minute, then large particles were removed by squeezing the mixture through four layers of cheesecloth. For treated cohorts, freshly prepared inoculum was used same day. The control inocula were prepared by autoclaving the rumen content. The trial was carried out from birth to 8 weeks. The initial inoculum was administered within 3 days after birth, then at 2, 4, and 6 weeks after that. Calves were euthanized by penetrating captive bolt at 8-week of age and tissue collection immediately followed.

Tissues investigated in the study

All the calves were subjected to tissue collection. Caecum tissues were collected from each calf immediately after sacrifice. The epithelial layer of the caecum was collected. After being rinsed with 1X PBS to remove any digesta, tissues were cut with sterilized scalpels into small, 4–5 mm^2 fragments and put into Eppendorf safe-lock tubes. Collected tissues were snap-frozen in liquid nitrogen, then stored at −80 °C until further processing. For microbial community comparative analysis, we included sequence data previously published by our group from these tissue types: epithelial layer of the rumen (16), abomasum (17), ileum (18), and liver [15].

RNA extraction, quantification, and whole transcriptome sequencing

Caecum tissues were first homogenized using Precellys lysing beads CK28 (Bertin Technologies, France) at 6,800 RPM for 30 seconds for 4 times and the tissue homogenate was stored on ice in between cycles. An miRNeasy kit (Qiagen US) was used to extract total RNA samples using a QIAcube (Qiagen, US) with DNase treatment step added to the protocol. RNA 6000 Nano kit Agilent Technologies, US) was used to check the quality of extracted RNA. RNA samples with RNA integrity number ≥ 8.5 were quantified using Qubit 4.0 (Thermo Fisher, US) for sequencing library preparation.

Illumina TruSseq ribo-zero gold kit was used for RNA-sequencing library preparation according to manufacturer's instructions, with 1μg of total RNA as input for each sample. The quality of prepared libraries was analyzed by Bioanalyzer using a DNA 1000 kit (Agilent Technologies, US). Quantification of library was performed using Kapa quantification kit (Roche, Basel, Switzerland) using a QuantStudio 5 instrument (Applied Biosystems, USA). Initial pooling of the libraries was done using the quantification generated by the Kapa quantification kit by Illumina's pooling calculator (https://support.illumina.com/help/pooling-calculator/pooling-calculator.htm). The pooled libraries were sequenced using an Illumina

MiSeq Nano kit (Illumina, US). Library pooling was further normalized using the sample index ratio obtained from the Illumina MiSeq Nano kit to ensure equal quantity of eash sample in the pool before final sequencing. Final sequencing of pooled samples was done using an Illumina NextSeq high-output, 300-cycle cartridge on an Illumina NextSeq 500 instrument to generate paired-end, 2x150bp reads.

Power analysis of RNA sequencing

Minimal group sizes required for RNA sequencing were determined by a power analysis using the Bioconductor Package ssizeRNA (34). It was determined that 4 biological replicates per treatment with 20 million reads per sample would be sufficient to identify differentially expressed genes from RNA-sequencing data at a power of 0.90 using the following parameters: statistical power cutoff = 0.8, number of genes = 20,000, minimum number of DEGs = 200, average read count = 1000, fold change = 2, FDR = 0.05. We obtained 50-60 million reads per sample in our experiment design. Thus, the sequencing depth would ensure sufficient statistical power for transcriptome analysis.

Mapping of RNA sequencing raw reads and differential gene expression analysis

For sequence alignment, NCBI ARS-UCD1.3 (https://www.ncbi.nlm.nih.gov/assembly/GCF_002263795.2), *Bos taurus* reference genome was used. For each sample, raw reads were aligned using STAR (35). Using gene-level, raw-read counts as the input, differentially expressed genes (DEGs) were identified using DESeq2 (36), with *p*-values corrected for multiple testing using the Benjamini-Hochberg method (37). To identify confident DEGs, combinatory cutoffs were used to filter DEGs: *p*-value ≤ 0.05, fold-change ≥ 2 and mean RC ≥ 10. Normalized read count, FPKM (fragments per kilobase of transcript per million reads mapped), was calculated using cufflinks (38). Genes were considered

expressed, if the FPKM value is 1 or more. Gene function annotation and gene ontology (GO) analysis were performed using DAVID (39).

Reverse transcriptase qPCR (RT-qPCR) verification of RNA sequencing results

Six randomly selected DEGs identified by RNAseq were analyzed for expression analysis using reverse transcription quantitative PCR (RT-qPCR): *GEM, LRP11*, *KITLG*, *MCOLN3*, *PLCXD3* and *IFITM3*. *GEM* encodes a protein that is part of the RAD/GEM family of GTP-binding proteins. Associated with the inner face of the plasma membrane, GEM functions as a regulatory protein in receptor-mediated signal transduction (40). The protein encoded by *LRP11* is predicted be an integral component of membrane, and it plays a central role in leptin signaling and regulation of energy homeostasis (41). *KITLG* has a reported role in cell migration and proliferation (42). MCOLN3 protein is a member of the mucolipin family of ion channels, and a novel regulator of trafficking along the endosomal pathway (43, 44). Reduced expression of *PLCXD3* is associated with disruption of glucose sensing and insulin signaling in pancreatic β-cells (45). IFITM3 protein was reported as an important innate immune effector that prevent diverse virus infections in vertebrates (46).

cDNA synthesis was performed using 2 μg of RNA with High-Capacity cDNA master mix (Life technologies). Gene-specific, Taqman assay probes were ordered from ThermoFisher (ThermoFisher Scientific, US). All real-time qPCR reactions were performed using the QuantStudio 5 (ThermoFisher Scientific, US). The qPCR cycling parameter was set as follows: one step of Uracil-DNA glycosylases treatment at 50°C for 2 min, then a denaturation/activation step at 95 °C for 2 min, followed by 40 cycles of 95 °C for 15s and 60 °C for 60s. Triplicate reactions were carried out for each target gene. Gene expression level was normalized to two reference genes, *ACTB* and *HMBS*, which were reported with high stability in cattle (47). The relative quantification of gene expression was determined using the $2^{-\Delta\Delta Ct}$ method (48).

Taxonomic classification of caecum community using ribosomal RNA (rRNA)-sequencing reads

For all the tissue types, rRNA reads from the host microbial community was extracted computationally by the following steps: 1) The total raw reads generated from the RNA-sequencing of the host tissue were first mapped to the genome of *Bos taurus* (NCBI, ARS-UCD 1.3) using STAR (35); 2) To enrich rRNA reads, the unmapped reads (non-cattle RNA-seq raw reads) were mapped to rRNA reference using SortMeRNA (49), using the rRNA reference provided by SortMeRNA. 3) The aligned rRNA reads were followed for microbial taxonomic classification, using Kraken (50) (http://ccb.jhu.edu/software/kraken/MANUAL.html). The Kraken database used in the analysis contained ~25,000 complete bacterial, archaeal, and viral genomes in RefSeq.

Differential abundance analysis of microbial genera and expression association between host genes and microbial genera

Genus levels, raw read-counts were used to access the microbial community differences between the treated and control groups using DESeq2 (36), with p-values corrected for multiple testing using the Benjamini-Hochberg method (37). To identify differentially abundant genera (DAG) with high confidence, the following filtering criteria were applied: fold-change ≥ 2 and p-value < 0.05. Clustering analysis was performed using normalized read-count at genus level with prcomp in R (version 3.2).

To identify the host genes with significant association with its microbes, Spearman'rho analysis was done (SciPy v1.2.0) using the normalized read counts of caecum mRNA and its epimural microbial rRNA. Before the association analysis, we normalized the genus-level read-counts by the following steps 1) Calculating the per-million-factor (PMF) by dividing the total

number of reads mapped to genus level by 1,000, 000; 2) The raw read-count at genus level was divided by PMF to get normalized read-count. Only genera with a mean normalized read count less than 5 across all samples were considered for further analysis. DEGs in the caecum were included in the association analysis. To determine statistical significance, these cutoff values were used: P-values ≤ 0.0001 and the correlation coefficient absolute value more than 0.8.

Comparative analysis of microbial communities in different tissue types

Microbial communities were compared across the rumen, ileum, abomasum, and caecum. For each tissue type, microbial taxa at genus level were included for the analysis. Principal component analysis was performed by including all the tissue types for each treatment group. The top 5% most abundant genera were identified for each tissue type for the treated group, using mean, normalized read count for each genus. Then the shared genera between rumen, ileum, abomasum, and caecum samples were identified. Their abundance in each tissue type was graphed with a stacked bar graph.

Results

RNA quality, sequencing reads and total number of expressed genes

On average, a total of 48.1 ± 0.85M reads was obtained for each of the sample. The average mapping rate is 83.11 ± 0.77%. An average of 10,243 ± 341 genes were expressed (FPKM ≥ 1) for each sample. For microbial classification, an average of 2.35 ± 0.17M reads were successfully classified by Kraken. RT-qPCR analysis confirmed the expression profiles as identified by the RNA sequencing method (**Figure 1**).

Gene expression analysis and associated pathways

A total of 1,836 genes were identified as significantly differentially expressed (*p*-value ≤ 0.05,

fold-change ≥2 and mean RC ≥ 10) between the treated and control groups. Of these, 86 of them had increased expression and 1,750 of them had decreased expression in the treated group compared to the control. GO analysis using the up-regulated genes in the treated group indicated that these genes were enriched in the pathways related to cell proliferation (**Figure 2A**). For down-regulated genes in the treated group, a significant enrichment in the immune response, host response to pathogens, and inflammatory responses was observed (**Figure 2B**). Ten genes were identified as the top 10 mostly highly expressed genes in the caecum in the treated group, *RMRP*, *SPINK1*, *EBD*, *LYSB*, *OLFM4*, *CYTB*, *ACTG2*, *TPT1*, *SPINK4*, and *PIGR*. Gene ontology analysis indicated that these genes were enriched in the cellular component (GO: 0005576; 5 genes, *p*-value < 0.001). *PIGR* encodes a transmembrane protein, which facilitates the transcytosis of the soluble polymeric isoforms of immunoglobulin A and immunoglobulin M in immune complexes (51).

rRNA transcriptome analysis of caecum microbial community and associated host mRNA expression changes

In the caecum, 582 genera were identified with a raw, mean read counts of 5 or more, and 343 genera were identified as DAGs (fold-change ≥ 2 and *p*-value < 0.05). Among the DAGs, 129 of them showed significant increase in abundance in the treated group, while 214 of them showed significant decrease in the treated group. For the genera with significant abundance increase in the treated group, the top 15 most abundant belonged to two phyla: Bacillota and Pseudomonadota (**Figure 3**).

A total of 56 DEGs showed significant association with 20 or more genera in the caecum. Eight of these genes had significant association with more than 40 genera. These genes include *RAB26*, *SLC16A11*, *RAP1GAP*, *REEP6*, *TMEM190*, *BOLA-DQB*, *TSPAN32*, and *CA7*.

Reactome pathway analysis indicated the enrichment of these genes in the following pathways: Rap1 signaling (BTA-392517, 2 genes, $p < 0.01$), integrin signaling (BTA-354192, 2 genes, $p < 0.01$), MHC class II antigen presentation (BTA-2132295, 2 genes, $p < 0.02$), and adaptive immune system (BTA-1280218, 4 genes, $p < 0.01$).

Microbial community profiles of different GI tissue types

In this study, we analyze the microbial community profile of all the GI tissues we collected from the same set of calves. For both treatments, we observed a clear separation between liver and the other tissues, though the other tissues appear to be mixed under the control condition (**Figure 4a and Figure 4b**). For the treated group, the separation of tissue types is clear for the liver, rumen, and caecum. And there is no clear separation between the ileum and abomasum. (**Figure 5a and Figure 5b**). Within the treated group, a total of 20 genera, belonging to 7 phyla, were identified as commonly shared amongst rumen, ileum, abomasum, and caecum tissues. However, the abundance of these genera was significantly different ($p < 0.05$) among these tissues as shown in the stacked bar graph (**Figure 6**). The phylum of Bacillota had the highest number of genera shared among these tissue types.

Discussion

The microbial community might interact with the host to affect immune development at the caecum level

For the DEGs associated with the highest number of microbes, GO analysis indicated an enrichment pathway associated with inflammation and immune response. The Rap1 signaling pathway is involved in diverse processes, including cell adhesion, cell-cell junction formation, and cell polarity. Rap1 is a member of the Ras-like small GTPases. It plays a role in the integrin signaling pathway (52), and functions as a regulator of morphogenesis *in vivo* (53). Integrins

belong to a family of ubiquitous αβ heterodimeric receptors, which exist in multiple conformations and interact with a diverse range of ligands. Additionally, integrins mediate the interactions between cytoskeleton and the extracellular matrix, and they play essential roles in inflammation, infection, and angiogenesis (54-56). In human studies, it is suggested that the caecum contributes to gut homeostasis and is a major site for generating IgA-secreting cells (57). Subsequently, secretory IgA cells play a significant role in regulating commensal bacteria populations in animal models (58-60). The precise role of caecum in host immune system is unknown in cattle. Our findings provided empirical evidence that the microbial communities in the caecum may interact with the host extensively to impact the development of the host's immune system. Our experiment was done in newborn calves, in which the immune system is immature. Thus, this might be an ideal window to manipulate host immunity and gut microbe colonization through artificial dosing.

The impact of artificial dosing on the caecum development captured by the whole transcriptome sequencing

As part of the lower gut, caecum is largely ignored in dairy nutrition studies. However, published studies reported significant contributions of the lower gut to host production efficiency (61-63) and immune system maturation (64, 65). In non-ruminants, the interaction between the gut-associated lymphoid tissues (GALT) and gastrointestinal (GIT) microbiota affected the functional development of the immune system (66, 67). The stratified keratinized squamous epithelial cells make rumen great for absorption. However, rumen lacks the immunological functionality of the mucosal epithelium present in other regions of the GI tract (68). GALT is one of the most important immunological tissues since it represents nearly 70% of all the lymphoid tissue (69). The complete maturation of the GALT tissue is largely dependent on the

interaction with GIT microbes (69). In our study, the downregulated genes in the treated group showed an enrichment in immune response. This finding suggested that the immune response in the epithelial layer of the caecum was impacted by the artificial dosing. Our study only included one type of inoculant with a fixed dosing schedule. The next logical step for follow-up studies will be to investigate if the dosing content and frequency affect or enhance the expression patterns of the immunity related genes in the caecum. The most critical would be to find the core set of microbes that show consistent association with the expression changes in immunity related genes in the host. This set of core microbes may help the development of refined dosing strategy with targeted response.

For the top 10 most highly expressed genes in the treated group, they showed an enrichment in cellular component. This finding indicates that artificial dosing impacted cell structure and proliferation in the caecum. The caecum is a site for generating IgA-secreting cells as reported in human studies. The highly abundant expression of *PIGR* identified in our study is consistent with the findings in humans (51). *LYSB* encodes an intestinal lysozyme with lipolytic activity, which is involved in the disruption of the mycobacteria outer membrane (70, 71). Lysozyme has strong bacteriolytic efficacy and function as defense enzymes against bacterial infections (72). Thus, the lysozyme is considered an important part of the innate immune system due to its strong antimicrobial activities against bacterial, fungal and viral pathogens (73). Additionally, in ruminants and animals with foregut fermentation (74), the lysozymes function as a digestion enzyme that degrades the foregut bacteria as a source of amino acids (75). In our study, the high expression of *LYSB* in the caecum, a part of the lower gut, might have a dual function in defending the host from the influx of foreign microbes introduced by the artificial dosing, and digesting the excessive number of microbes that are normally not present in calves reared by conventional practice. Consistent with this, Domínguez-Bello et al. reported the activity of

bovine gastric lysozyme against pure bacterial cultures (76). Thus, it's possible that the high expression of *LYSB* in the caecum help the host defend against potential infection resultant from the artificial dosing.

Selective retention of microbes in the GI tract after dosing treatment

Following birth, all regions of the GI tract in the calf undergo microbe acquisition and colonization. Studies have shown that the microbiome diversity and composition differ by region and developmental stage throughout different regions of the GI tract (77-82) and biogeographically (through space and time) (Michelland et al. 2009; Yeoman et al. 2018; Bi et al. 2019; Zhuang et al. 2020). We identified 20 genera, belonging to 7 phyla, that are shared between the different GI tissue types investigated in this study. However, the abundance of these genera is significantly different amongst the tissue types included in this study. Thus, it's evident that the same dosing strategy can lead to differential microbial community in different locations of the gut. This might largely be dependent on the local physiological and ecological environment of the GI tract.

The important role of rumen microbiome in host nutrient use efficiency and production traits has been explored extensively (83-91). However, studies indicated that feed intake and types have a significant impact shaping ruminal microbiome diversity (90, 92, 93), making it difficult to assess the exact contribution of rumen microbiome to host production efficiency traits. When investigating the lower gut microbiome and its relationship to host feed efficiency and production traits, Monteiro and co-authors indicated that the lower gut microbiome diversity is less dependent on feed intake and is associated with enhanced ability to digest dietary nutrients. Thus, Monteiro and co-authors suggested that lower gut microorganisms might be correlated with the host milk production traits more than previously appreciated (61). For future dosing experiments, varied inoculants and dosing schedule may help identify the core set of

microbes that persist in the lower gut. And from this group, further analysis that links the host production efficiency and the caecal microbial community can help identify the caecal microbes with a reliable association with host production efficiency traits.

Acknowledgments

We thank Andrea Edwards for helping with the tissue sample processing and cataloging. The farm crew at the US Dairy Forage Research Center helped with day-to-day calf management.

References (Vancouver or NLM style)

References cited

1. Rey M, Enjalbert F, Combes S, Cauquil L, Bouchez O, Monteils V. Establishment of ruminal bacterial community in dairy calves from birth to weaning is sequential. J Appl Microbiol. 2014;116:245-57.

2. Diao Q, Zhang R, Fu T. Review of Strategies to Promote Rumen Development in Calves. Animals (Basel). 2019;9(8).

3. Yanez-Ruiz DR, Macias B, Pinloche E, Newbold CJ. The persistence of bacterial and methanogenic archaeal communities residing in the rumen of young lambs. FEMS Microbiol Ecol. 2010;72(2):272-8.

4. De Barbieri I, Hegarty RS, Silveira C, Gulino LM, Oddy VH, Gilbert RA, et al. Programming rumen bacterial communities in newborn Merino lambs. Small Ruminant Res. 2015;129:48-59.

5. Krehbiel CR, Rust SR, Zhang G, Gilliland SE. Bacterial direct-fed microbials in ruminant diets: Performance response and mode of action. J Anim Sci. 2003;81:E120-E32.

6. Hong HA, Duc LH, Cutting SM. The use of bacterial spore formers as probiotics. Fems Microbiology Reviews. 2005;29(4):813-35.

7. Kumar U, Sareen VK, Singh S. Effect of Saccharomyces-Cerevisiae Yeast Culture Supplement on Ruminal Metabolism in Buffalo Calves Given a High Concentrate Diet. Anim Prod. 1994;59:209-15.

8. Xiao JX, Alugongo GM, Chung R, Dong SZ, Li SL, Yoon I, et al. Effects of Saccharomyces cerevisiae fermentation products on dairy calves: Ruminal fermentation, gastrointestinal morphology, and microbial community. J Dairy Sci. 2016;99(7):5401-12.

9. Yanez-Ruiz DR, Abecia L, Newbold CJ. Manipulating rumen microbiome and fermentation through interventions during early life: a review. Front Microbiol. 2015;6.

10. Abecia L, Martin-Garcia AI, Martinez G, Newbold CJ, Yanez-Ruiz DR. Nutritional intervention in early life to manipulate rumen microbial colonization and methane output by kid goats postweaning. J Anim Sci. 2013;91(10):4832-40.

11. Abecia L, Waddams KE, Martinez-Fernandez G, Martin-Garcia AI, Ramos-Morales E,

Newbold CJ, et al. An Antimethanogenic Nutritional Intervention in Early Life of Ruminants Modifies Ruminal Colonization by Archaea. Archaea. 2014;2014.

12. DePeters EJ, George LW. Rumen transfaunation. Immunol Lett. 2014;162(2 Pt A):69-76.

13. Steiner S, Linhart N, Neidl A, Baumgartner W, Tichy A, Wittek T. Evaluation of the therapeutic efficacy of rumen transfaunation. J Anim Physiol Anim Nutr (Berl). 2020;104(1):56-63.

14. Rager KD, George LW, House JK, DePeters EJ. Evaluation of rumen transfaunation after surgical correction of left-sided displacement of the abomasum in cows. J Am Vet Med Assoc. 2004;225(6):915-20.

15. Zhong RZ, Sun HX, Li GD, Liu HW, Zho DW. Effects of inoculation with rumen fluid on nutrient digestibility, growth performance and rumen fermentation of early weaned lambs. Livestock Science. 2014;162:154-8.

16. Li W, Edwards A, Riehle C, Cox MS, Raabis S, Skarlupka JH, et al. Transcriptomics analysis of host liver and meta-transcriptome analysis of rumen epimural microbial community in young calves treated with artificial dosing of rumen content from adult donor cow. Sci Rep. 2019;9(1):790.

17. Gaowa N, Li W, Murphy B, Cox MS. The Effects of Artificially Dosed Adult Rumen Contents on Abomasum Transcriptome and Associated Microbial Community Structure in Calves. Genes (Basel). 2021;12(3).

18. Li W, Edwards A, Cox MS, Raabis SM, Skarlupka JH, Steinberger AJ, et al. Changes in the host transcriptome and microbial metatranscriptome of the ileum of dairy calves subjected to artificial dosing of exogenous rumen contents. Physiol Genomics. 2020;52(8):333-46.

19. Nath MC, Meghal SK. Effect of carbohydrates on the intestinal synthesis of thiamine in rats. Biochem J. 1961;81:220-4.

20. Burkholder PR, McVeigh I. Synthesis of vitamins by intestinal bacteria. Proc Natl Acad Sci U S A. 1942;28:285-9.

21. Gressley TF, Hall MB, Armentano LE. Ruminant Nutrition Symposium: Productivity, digestion, and health responses to hindgut acidosis in ruminants. J Anim Sci. 2011;89(4):1120-30.

22. Oh JH, Hume ID. Development of microbial activity in the alimentary tract of lambs. Journal of Animal Science. 1972;35:450-9.

23. Van Soest PJ. Nutritional Ecology of the Ruminant, 2nd Edition. Comstock: Ithaca, xii. 1994:476.

24. Neubauer V, Petri RM, Humer E, Kroger I, Reisinger N, Baumgartner W, et al. Starch-Rich Diet Induced Rumen Acidosis and Hindgut Dysbiosis in Dairy Cows of Different Lactations. Animals (Basel). 2020;10(10).

25. Reynolds CK. Production and metabolic effects of site of starch digestion in dairy cattle. Anim Feed Sci Technol 2006;130:78-94.

26. Emmanuel DG, Madsen KL, Churchill TA, Dunn SM, Ametaj BN. Acidosis and lipopolysaccharide from Escherichia coli B:055 cause hyperpermeability of rumen and colon tissues. J Dairy Sci. 2007;90(12):5552-7.

27. Popova M, McGovern E, McCabe MS, Martin C, Doreau M, Arbre M, et al. The Structural and Functional Capacity of Ruminal and Cecal Microbiota in Growing Cattle Was Unaffected by Dietary Supplementation of Linseed Oil and Nitrate. Front Microbiol. 2017;8.

28. Godoy-Vitorino F, Goldfarb KC, Karaoz U, Leal S, Garcia-Amado MA, Hugenholtz P, et al. Comparative analyses of foregut and hindgut bacterial communities in hoatzins and cows. ISME J. 2012;6(3):531-41.

29. Sicilianojones J, Murphy MR. Production of Volatile Fatty-Acids in the Rumen and Cecum-Colon of Steers as Affected by Forage - Concentrate and Forage Physical Form. Journal of Dairy Science. 1989;72(2):485-92.

30. Jewell KA, McCormick CA, Odt CL, Weimer PJ, Suen G. Ruminal Bacterial Community Composition in Dairy Cows Is Dynamic over the Course of Two Lactations and Correlates with Feed Efficiency. Appl Environ Microbiol. 2015;81(14):4697-710.

31. Connor EE, Hutchison JL, Olson KM, Norman HD. Triennial Lactation Symposium: Opportunities for improving milk production efficiency in dairy cattle. J Anim Sci. 2012;90(5):1687-94.

32. Council NR. Nutrient requirements of dairy cattle, 7th revised ed. National Academy Press, Washington DC. 2001.

33. Jewell KA, McCormick CA, Odt CL, Weimer PJ, Suen G. Ruminal Bacterial Community Composition in Dairy Cows Is Dynamic over the Course of Two Lactations and Correlates with Feed Efficiency. Applied and Environmental Microbiology. 2015;81(14):4697-710.

34. Bi R, Liu P. Sample size calculation while controlling false discovery rate for differential expression analysis with RNA-sequencing experiments. Bmc Bioinformatics. 2016;17.

35. Dobin A, Davis CA, Schlesinger F, Drenkow J, Zaleski C, Jha S, et al. STAR: ultrafast universal RNA-seq aligner. Bioinformatics. 2013;29(1):15-21.

36. Love MI, Huber W, Anders S. Moderated estimation of fold change and dispersion for RNA-seq data with DESeq2. Genome Biol. 2014;15(12):550.

37. Benjamini Y, Hochberg Y. Controlling the False Discovery Rate - a Practical and Powerful Approach to Multiple Testing. J R Stat Soc B. 1995;57(1):289-300.

38. Trapnell C, Roberts A, Goff L, Pertea G, Kim D, Kelley DR, et al. Differential gene and transcript expression analysis of RNA-seq experiments with TopHat and Cufflinks. Nat Protoc. 2012;7(3):562-78.

39. Jiao X, Sherman BT, Huang da W, Stephens R, Baseler MW, Lane HC, et al. DAVID-WS: a stateful web service to facilitate gene/protein list analysis. Bioinformatics. 2012;28(13):1805-6.

40. Ward Y, Yap SF, Ravichandran V, Matsumura F, Ito M, Spinelli B, et al. The GTP binding proteins Gem and Rad are negative regulators of the Rho-Rho kinase pathway. J Cell Biol. 2002;157(2):291-302.

41. Liu Q, Zhang J, Zerbinatti C, Zhan Y, Kolber BJ, Herz J, et al. Lipoprotein Receptor LRP1 Regulates Leptin Signaling and Energy Homeostasis in the Adult Central Nervous System (vol 9, e1000575, 2011). Plos Biol. 2019;17(6).

42. Yang ZY, Liu SN, Wang YG, Chen Y, Zhang P, Liu YM, et al. High expression of KITLG is a new hallmark activating the MAPK pathway in type A and AB thymoma. Thorac Cancer. 2020;11(7):1944-54.

43. Martina JA, Lelouvier B, Puertollano R. The Calcium Channel Mucolipin-3 is a Novel Regulator of Trafficking Along the Endosomal Pathway. Traffic. 2009;10(8):1143-56.

44. Lelouvier B, Puertollano R. Mucolipin-3 regulates luminal calcium, acidification, and

membrane fusion in the endosomal pathway. J Biol Chem. 2011;286(11):9826-32.

45. Aljaibeji H, Mukhopadhyay D, Mohammed AK, Dhaiban S, Hachim MY, Elemam NM, et al. Reduced Expression of PLCXD3 Associates With Disruption of Glucose Sensing and Insulin Signaling in Pancreatic beta-Cells. Front Endocrinol. 2019;10.

46. Spence JS, He RN, Hoffmann HH, Das T, Thinon E, Rice CM, et al. IFITM3 directly engages and shuttles incoming virus particles to lysosomes. Nature Chemical Biology. 2019;15(3):259-+.

47. Die JV, Baldwin RL, Rowland LJ, Li R, Oh S, Li C, et al. Selection of internal reference genes for normalization of reverse transcription quantitative polymerase chain reaction (RT-qPCR) analysis in the rumen epithelium. PLoS One. 2017;12(2):e0172674.

48. Livak KJ, Schmittgen TD. Analysis of relative gene expression data using real-time quantitative PCR and the 2(-Delta Delta C(T)) Method. Methods. 2001;25(4):402-8.

49. Kopylova E, Noe L, Touzet H. SortMeRNA: fast and accurate filtering of ribosomal RNAs in metatranscriptomic data. Bioinformatics. 2012;28(24):3211-7.

50. Wood DE, Salzberg SL. Kraken: ultrafast metagenomic sequence classification using exact alignments. Genome Biol. 2014;15(3):R46.

51. Turula H, Wobus CE. The Role of the Polymeric Immunoglobulin Receptor and Secretory Immunoglobulins during Mucosal Infection and Immunity. Viruses. 2018;10(5).

52. Bos JL, de Bruyn K, Enserink J, Kuiperij B, Rangarajan H, Rehmann H, et al. The role of Rap1 in integrin-mediated cell adhesion. Biochemical Society Transactions. 2003;31:83-4.

53. Asha H, de Ruiter ND, Wang MG, Hariharan IK. The Rap1 GTPase functions as a regulator of morphogenesis in vivo. Embo J. 1999;18(3):605-15.

54. Dong X, Hudson NE, Lu C, Springer TA. Structural determinants of integrin beta-subunit specificity for latent TGF-beta. Nat Struct Mol Biol. 2014;21(12):1091-6.

55. von Andrian UH, Chambers JD, McEvoy LM, Bargatze RF, Arfors KE, Butcher EC. Two-step model of leukocyte-endothelial cell interaction in inflammation: distinct roles for LECAM-1 and the leukocyte beta 2 integrins in vivo. Proc Natl Acad Sci U S A. 1991;88(17):7538-42.

56. Lammermann T, Bader BL, Monkley SJ, Worbs T, Wedlich-Soldner R, Hirsch K, et al. Rapid leukocyte migration by integrin-independent flowing and squeezing. Nature. 2008;453(7191):51-5.

57. Masahata K, Umemoto E, Kayama H, Kotani M, Nakamura S, Kurakawa T, et al. Generation of colonic IgA-secreting cells in the caecal patch. Nat Commun. 2014;5:3704.

58. Suzuki K, Meek B, Doi Y, Muramatsu M, Chiba T, Honjo T, et al. Aberrant expansion of segmented filamentous bacteria in IgA-deficient gut. Proc Natl Acad Sci U S A. 2004;101(7):1981-6.

59. Peterson DA, McNulty NP, Guruge JL, Gordon JI. IgA response to symbiotic bacteria as a mediator of gut homeostasis. Cell Host & Microbe. 2007;2(5):328-39.

60. Strugnell RA, Wijburg OL. The role of secretory antibodies in infection immunity. Nat Rev Microbiol. 2010;8(9):656-67.

61. Monteiro HF, Zhou Z, Gomes MS, Peixoto PMG, Bonsaglia ECR, Canisso IF, et al. Rumen and lower gut microbiomes relationship with feed efficiency and production traits throughout the lactation of Holstein dairy cows. Sci Rep. 2022;12(1):4904.

62. Myer PR, Freetly HC, Wells JE, Smith TPL, Kuehn LA. Analysis of the gut bacterial communities in beef cattle and their association with feed intake, growth, and efficiency. Journal of Animal Science. 2017;95(7):3215-24.

63. Myer PR, Wells JE, Smith TP, Kuehn LA, Freetly HC. Microbial community profiles of the jejunum from steers differing in feed efficiency. J Anim Sci. 2016;94(1):327-38.

64. Mazmanian SK, Round JL, Kasper DL. A microbial symbiosis factor prevents intestinal inflammatory disease. Nature. 2008;453(7195):620-5.

65. Atarashi K, Tanoue T, Shima T, Imaoka A, Kuwahara T, Momose Y, et al. Induction of colonic regulatory T cells by indigenous Clostridium species. Science. 2011;331(6015):337-41.

66. Gray J, Oehrle K, Worthen G, Alenghat T, Whitsett J, Deshmukh H. Intestinal commensal bacteria mediate lung mucosal immunity and promote resistance of newborn mice to infection. Sci Transl Med. 2017;9(376).

67. Hu L, Geng S, Li Y, Cheng S, Fu X, Yue X, et al. Exogenous Fecal Microbiota

Transplantation from Local Adult Pigs to Crossbred Newborn Piglets. Front Microbiol. 2017;8:2663.

68. Graham C, Simmons NL. Functional organization of the bovine rumen epithelium. Am J Physiol Regul Integr Comp Physiol. 2005;288(1):R173-81.

69. Lopetuso LR, Scaldaferri F, Petito V, Gasbarrini A. Commensal Clostridia: leading players in the maintenance of gut homeostasis. Gut Pathog. 2013;5(1):23.

70. Gil F, Catalao MJ, Moniz-Pereira J, Leandro P, McNeil M, Pimentel M. The lytic cassette of mycobacteriophage Ms6 encodes an enzyme with lipolytic activity. Microbiology (Reading). 2008;154(Pt 5):1364-71.

71. Gil F, Grzegorzewicz AE, Catalao MJ, Vital J, McNeil MR, Pimentel M. Mycobacteriophage Ms6 LysB specifically targets the outer membrane of Mycobacterium smegmatis. Microbiology (Reading). 2010;156(Pt 5):1497-504.

72. Irwin DM. Evolution of cow nonstomach lysozyme genes. Genome. 2004;47:1082-90.

73. Ragland SA, Criss AK. From bacterial killing to immune modulation: Recent insights into the functions of lysozyme. Plos Pathog. 2017;13(9).

74. Yang Z. Likelihood ratio tests for detecting positive selection and application to primate lysozyme evolution. Mol Biol Evol. 1998;15(5):568-73.

75. Irwin DM, Wilson AC. Multiple cDNA sequences and the evolution of bovine stomach lysozyme. J Biol Chem. 1989;264(19):11387-93.

76. Dominguez-Bello MG, Pacheco MA, Ruiz MC, Michelangeli F, Leippe M, de Pedro MA. Resistance of rumen bacteria murein to bovine gastric lysozyme. BMC Ecol. 2004;4:7.

77. Mao SY, Zhang ML, Liu JH, Zhu WY. Characterising the bacterial microbiota across the gastrointestinal tracts of dairy cattle: membership and potential function. Scientific Reports. 2015;5.

78. Wang J, Fan H, Han Y, Zhao J, Zhou Z. Characterization of the microbial communities along the gastrointestinal tract of sheep by 454 pyrosequencing analysis. Asian-Australas J Anim Sci. 2017;30(1):100-10.

79. Perea K, Perz K, Olivo SK, Williams A, Lachman M, Ishaq SL, et al. Feed efficiency

phenotypes in lambs involve changes in ruminal, colonic, and small-intestine-located microbiota. J Anim Sci. 2017;95(6):2585-92.

80. Thomas M, Webb M, Ghimire S, Blair A, Olson K, Fenske GJ, et al. Metagenomic characterization of the effect of feed additives on the gut microbiome and antibiotic resistome of feedlot cattle. Sci Rep. 2017;7(1):12257.

81. Zhang H, Shao M, Huang H, Wang S, Ma L, Wang H, et al. The Dynamic Distribution of Small-Tail Han Sheep Microbiota across Different Intestinal Segments. Front Microbiol. 2018;9:32.

82. Chong CYL, Vatanen T, Oliver M, Bloomfield FH, O'Sullivan JM. The microbial biogeography of the gastrointestinal tract of preterm and term lambs. Scientific Reports. 2020;10(1).

83. Li FY, Guan LL. Metatranscriptomic Profiling Reveals Linkages between the Active Rumen Microbiome and Feed Efficiency in Beef Cattle. Applied and Environmental Microbiology. 2017;83(9).

84. Xue M, Sun H, Wu X, Guan LL, Liu J. Assessment of Rumen Microbiota from a Large Dairy Cattle Cohort Reveals the Pan and Core Bacteriomes Contributing to Varied Phenotypes. Appl Environ Microbiol. 2018;84(19).

85. Guan LL, Nkrumah JD, Basarab JA, Moore SS. Linkage of microbial ecology to phenotype: correlation of rumen microbial ecology to cattle's feed efficiency. FEMS Microbiol Lett. 2008;288(1):85-91.

86. Hernandez-Sanabria E, Goonewardene LA, Wang Z, Durunna ON, Moore SS, Guan LL. Impact of feed efficiency and diet on adaptive variations in the bacterial community in the rumen fluid of cattle. Appl Environ Microbiol. 2012;78(4):1203-14.

87. McCann JC, Wiley LM, Forbes TD, Rouquette FM, Tedeschi LO. Relationship between the Rumen Microbiome and Residual Feed Intake-Efficiency of Brahman Bulls Stocked on Bermudagrass Pastures. Plos One. 2014;9(3).

88. Myer PR, Smith TP, Wells JE, Kuehn LA, Freetly HC. Rumen microbiome from steers differing in feed efficiency. Plos One. 2015;10(6):e0129174.

89. Shabat SK, Sasson G, Doron-Faigenboim A, Durman T, Yaacoby S, Berg Miller ME, et al. Specific microbiome-dependent mechanisms underlie the energy harvest efficiency of ruminants. ISME J. 2016;10(12):2958-72.

90. Zhang Y, Li F, Chen Y, Wu H, Meng Q, Guan LL. Metatranscriptomic Profiling Reveals the Effect of Breed on Active Rumen Eukaryotic Composition in Beef Cattle With Varied Feed Efficiency. Front Microbiol. 2020;11:367.

91. McLoughlin S, Spillane C, Claffey N, Smith PE, O'Rourke T, Diskin MG, et al. Rumen Microbiome Composition Is Altered in Sheep Divergent in Feed Efficiency. Front Microbiol. 2020;11.

92. Pathak AK. Various factors affecting microbial protein synthesis in the rumen. Vet World. 2008;1(6):186-9.

93. Fliegerova KO, Podmirseg SM, Vinzelj J, Grilli DJ, Kvasnova S, Schierova D, et al. The Effect of a High-Grain Diet on the Rumen Microbiome of Goats with a Special Focus on Anaerobic Fungi. Microorganisms. 2021;9(1).

636 **Figure legend**

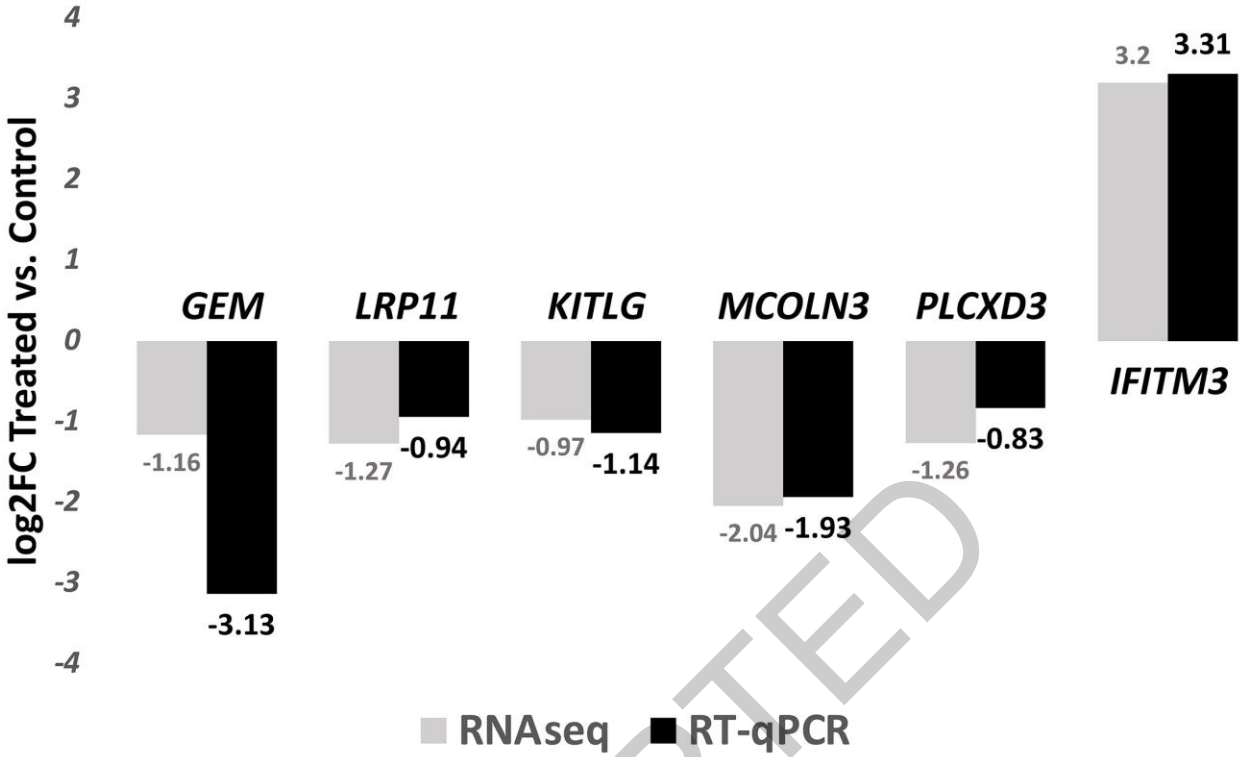

637

638 **Figure 1.** RT-qPCR analysis of selected genes. log2 transformed, fold-change values between

639 treated and control samples. Gray bars represent the values identified by RNAseq. Dark black

640 bars represent the values identified by RT-qPCR method.

641

642

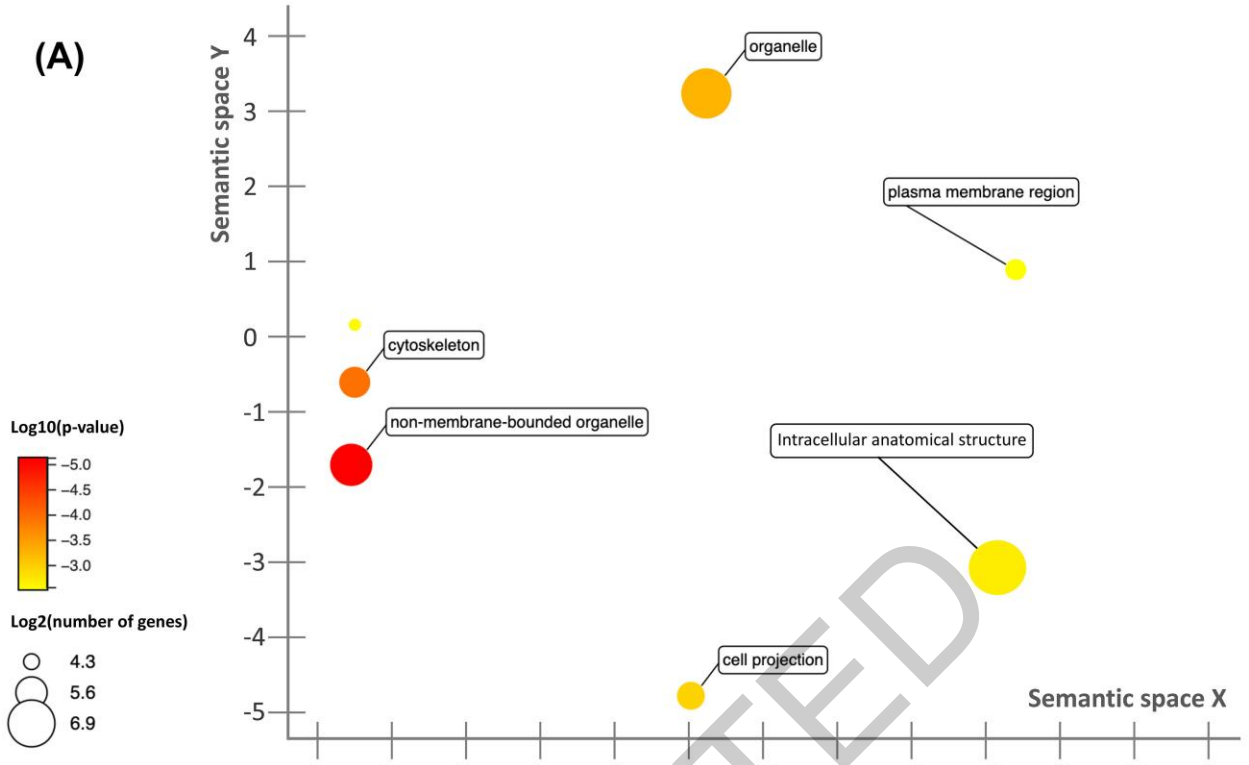

643

644

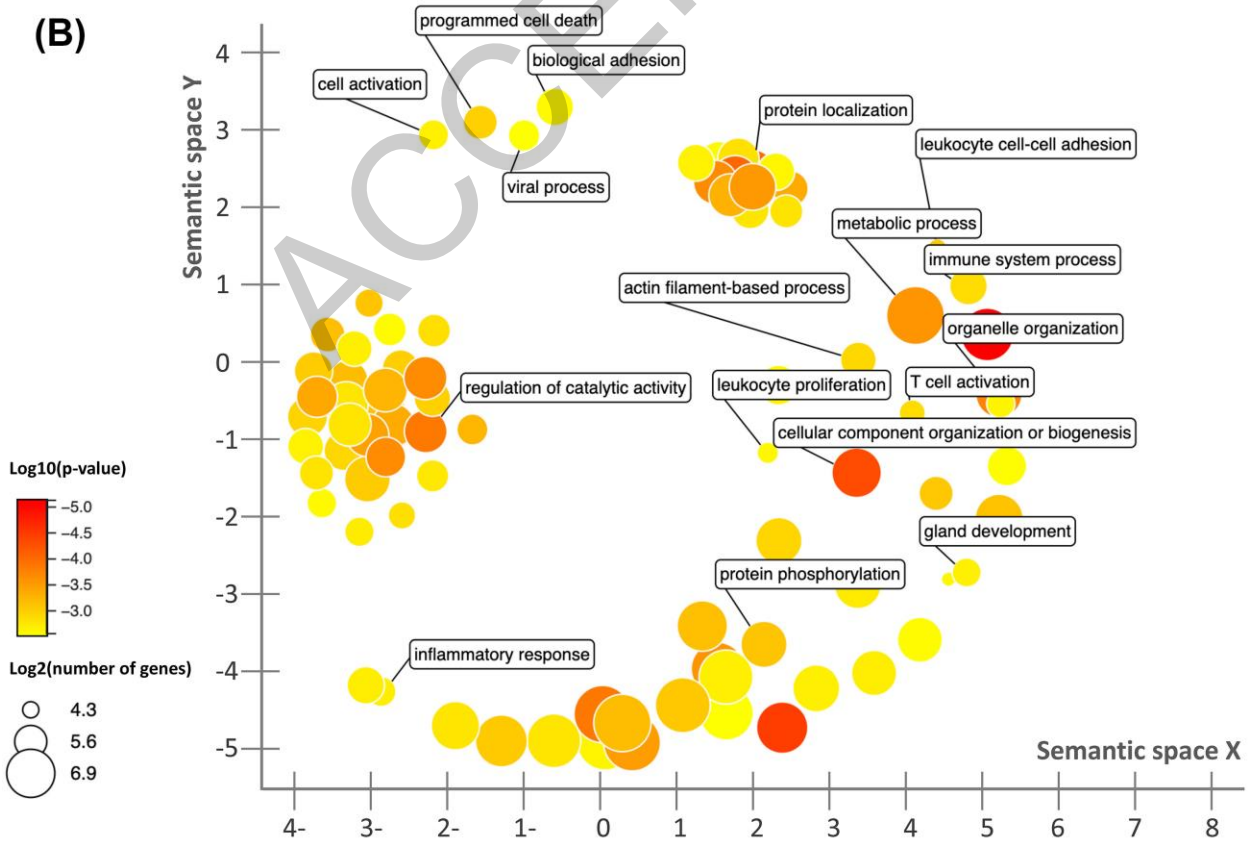

645

Figure 2. Gene ontology (GO) analysis of differential expressed genes between treated and control groups. **A.** GO analysis using the up-regulated genes in the treated group. **B.** GO analysis using down-regulated genes in the treated group. GO terms with similar functions are grouped together. The scale of log10 transformed p-value is represented by the yellow-orange bar on the bottom-left corner of the graph. The scale of the number of genes enriched for each GO terms is indicated by the circles on the bottom-left corner of the graph. The plot axes have no intrinsic meaning.

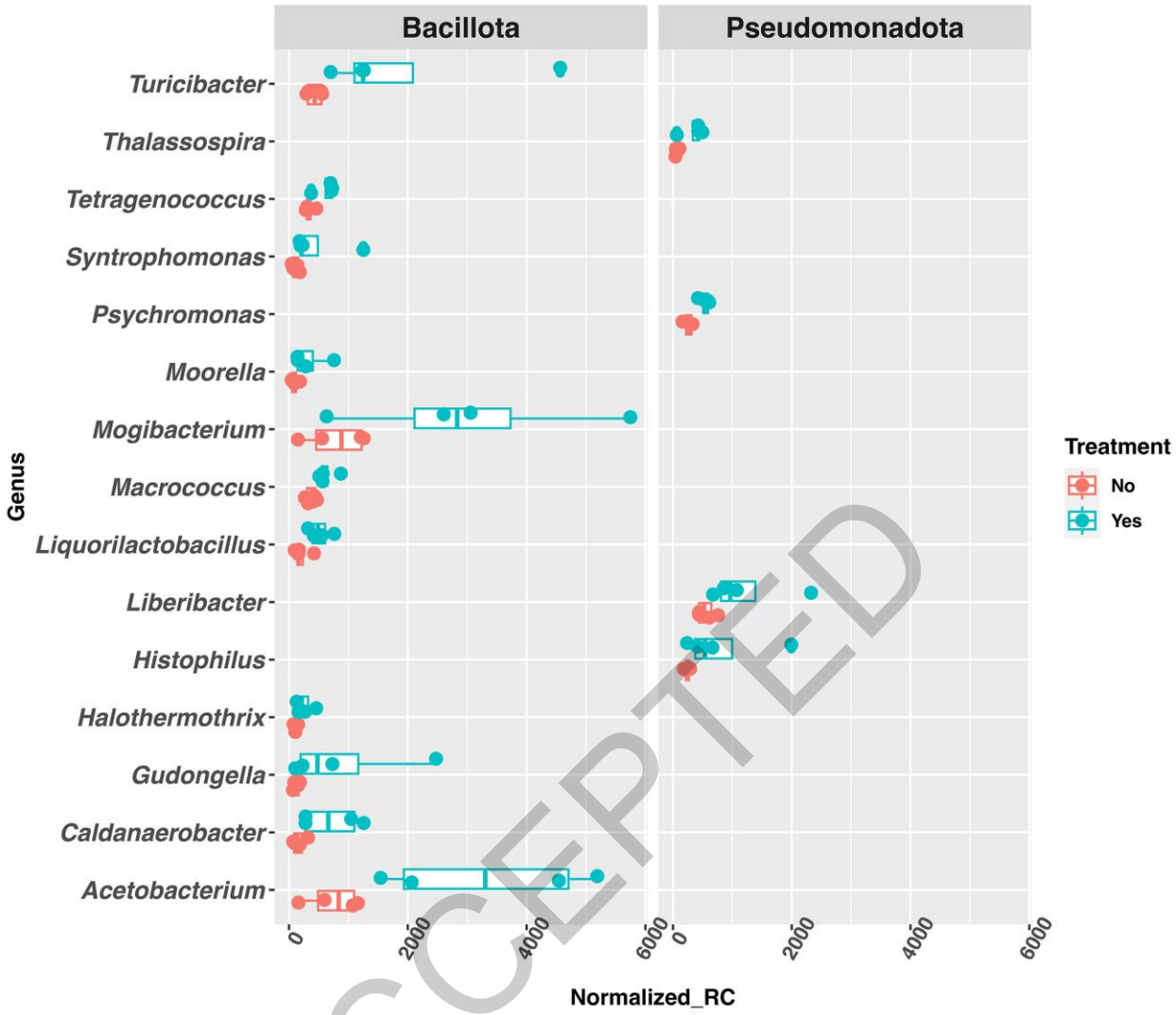

Figure 3. Boxplots of the read-counts for top 15 most abundant genera that showed significant increase in abundance in the treated group compared to the control in caecum. The genera are grouped by the phylum they belong.

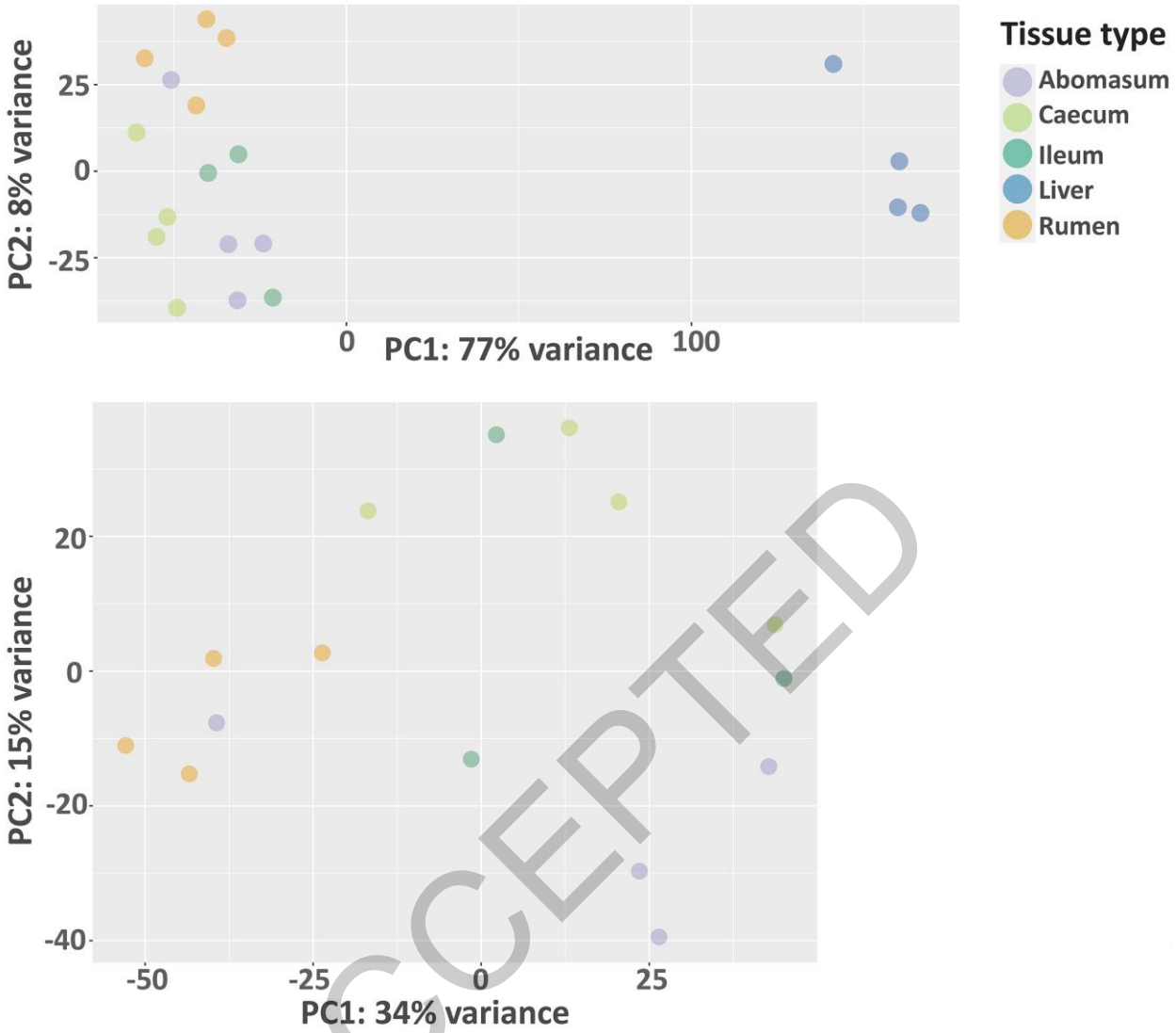

661

662 **Figure 4.** Principal component analysis (PCA) using the samples collected from the control

663 group. **A.** Samples collected from rumen, abomasum, ileum, liver and caecum are included in

664 the analysis. **B.** Non-liver samples are included in the analysis.

665

666

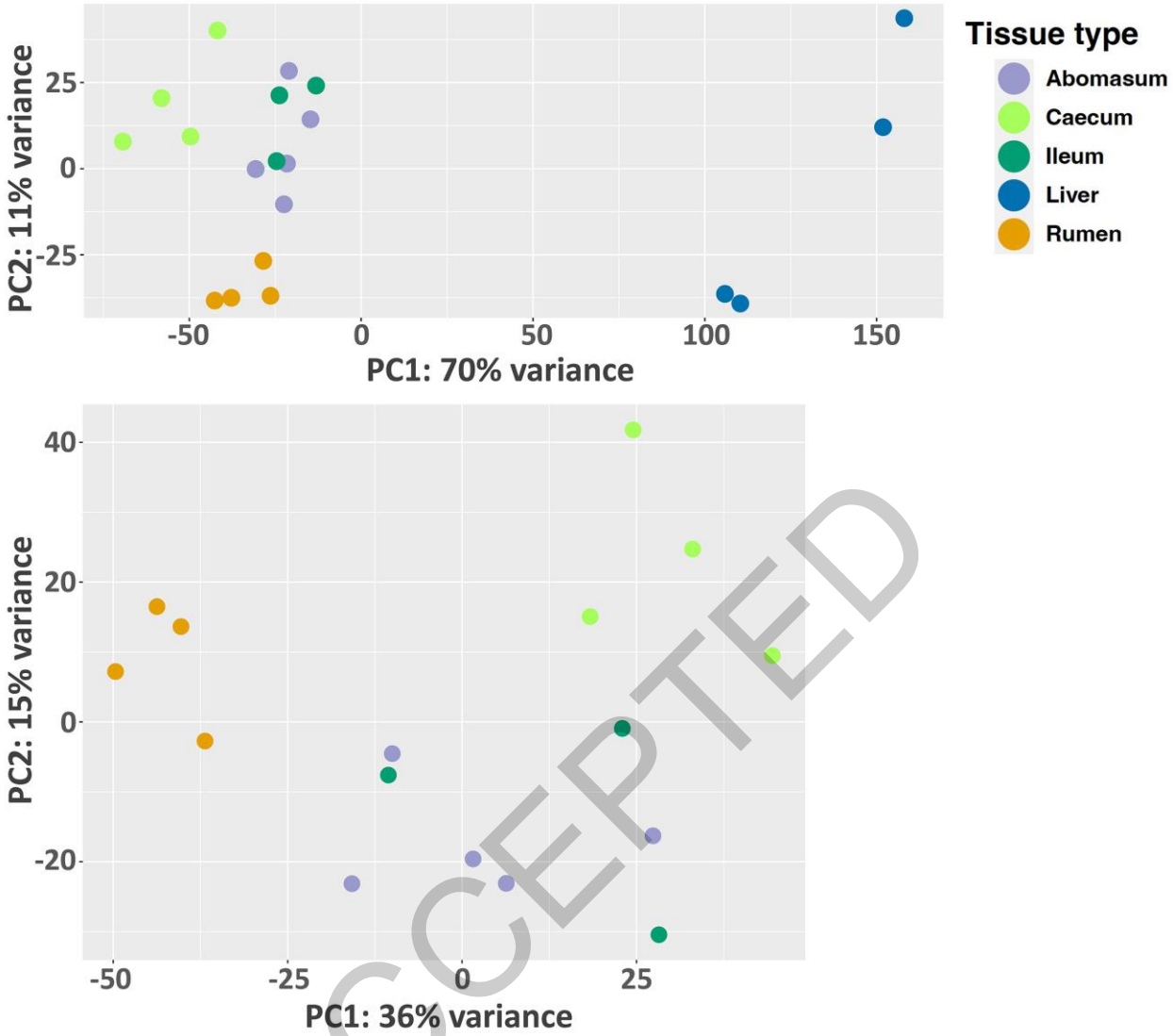

667

668 **Figure 5.** Principal component analysis (PCA) using the samples collected from the treated

669 group. **A.** Samples collected from rumen, abomasum, ileum, liver and caecum are included in

670 the analysis. **B.** Non-liver samples are included in the analysis.

671

672

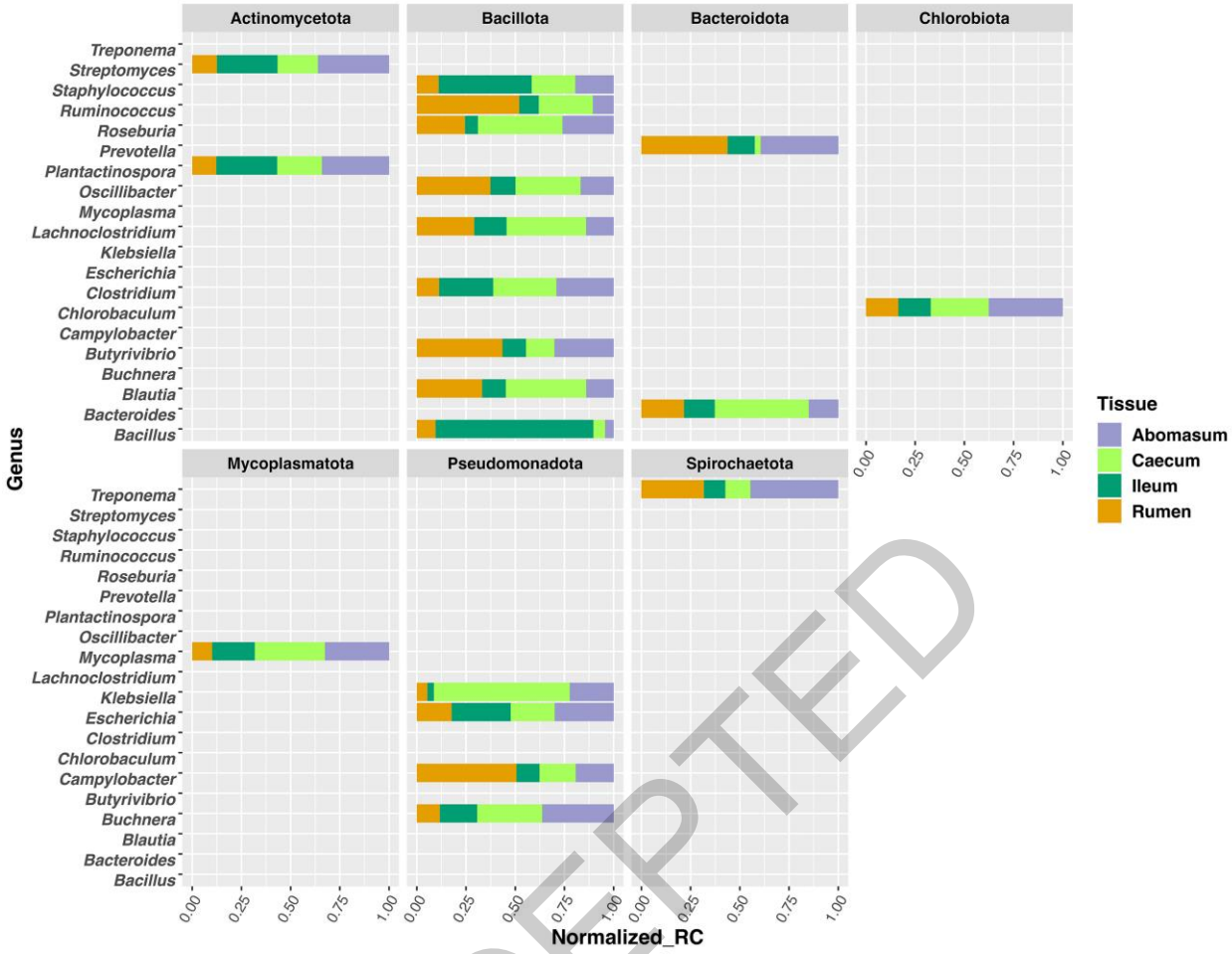

673

674 **Figure 6.** Stacked bar-chart showing the abundance distribution of 20 microbial genera shared

675 amongst rumen, ileum, abomasum, and caecum tissues. They genera are grouped by the phylum

676 they belong.

677
678